

**Resonant photoemission of single-crystal  $R\text{BaCo}_2\text{O}_{5+\delta}$  ( $R=\text{Gd}, \text{Dy}$ )**

W. R. Flavell,\* A. G. Thomas, D. Tsoutsou, A. K. Mallick, and M. North  
*Department of Physics, UMIST, P.O. Box 88, Manchester, M60 1QD United Kingdom*

E. A. Seddon, C. Cacho, A. E. R. Malins, and S. Patel  
*CLRC Daresbury Laboratory, Daresbury, Warrington, WA4 4AD United Kingdom*

R. L. Stockbauer, R. L. Kurtz, and P. T. Sprunger  
*Department of Physics, Louisiana State University, Baton Rouge, Louisiana 70803, USA*

S. N. Barilo, S. V. Shiryayev, and G. L. Bychkov  
*Institute of Solid State and Semiconductor Physics, Belarus Academy of Sciences, 17 P. Brovka St., Minsk 220072, Belarus*  
 (Received 6 July 2004; published 22 December 2004)

Resonant photoemission of single crystals of the double perovskites  $\text{GdBaCo}_2\text{O}_{5+\delta}$  and  $\text{DyBaCo}_2\text{O}_{5+\delta}$  has been carried out at the UK Synchrotron Radiation Source at Daresbury. The resonance onset energy at the Co  $3p \rightarrow 3d$  threshold is used to explore the Co spin state in the double perovskites as a function of temperature. In contrast with the simple perovskites  $\text{LaCoO}_3$  and  $\text{HoCoO}_3$ , an undelayed resonance is observed for  $\text{GdBaCo}_2\text{O}_{5+\delta}$  and  $\text{DyBaCo}_2\text{O}_{5+\delta}$  at temperatures as low as 50 K, consistent with the idea that the Co spin state in the pyramidal sites of the double perovskites does not fluctuate with temperature. The temperature variation of the data suggest that the phase transition observed in  $\text{GdBaCo}_2\text{O}_{5+\delta}$  at around 350 K is not associated with a sudden low spin-high spin switch in the octahedral sites. The giant rare earth ( $R$ )  $4d \rightarrow 4f$  resonances are also probed, and are used to identify the  $4f$  contributions to the valence band. This shows that the density of states close to the Fermi energy for all materials is of Co  $3d/O 2p$  character, with no  $R 4f$  contribution. Comparison is made with LSDA+U calculations. Our experiments indicate that the spin equilibrium in the double perovskites is significantly shifted in favor of higher spin multiplicities compared with materials such as  $\text{LaCoO}_3$ .

DOI: 10.1103/PhysRevB.70.224427

PACS number(s): 75.25.+z, 71.27.+a, 79.60.Bm

**INTRODUCTION**

The recently discovered “double perovskites,” of general formula  $R\text{BaCo}_2\text{O}_{5+\delta}$  ( $R$ =rare earth element,  $0 \leq \delta \leq 1$ ) show a range of poorly understood spin-state transitions.<sup>1</sup> The nominal Co valency varies between 3.5 ( $\delta=1$ ) and 2.5 ( $\delta=0$ ). When  $\delta=0.5$ , the Co valence is 3.0, and giant magnetoresistance may be observed.<sup>1</sup> The structure is derived from the “112” structure of  $\text{YBaFeCuO}_5$ <sup>2</sup> and is formed from the stacking sequence  $[\text{CoO}_2][\text{BaO}][\text{CoO}_2][\text{LnO}_\delta]$  along the  $c$  direction. Whereas the Co (III) ion occupies only octahedral sites ( $\text{CoO}_6$ ) in simple perovskites such as  $\text{LaCoO}_3$ , in the double perovskites, Co (III) is present in two environments, octahedral and pyramidal ( $\text{CoO}_5$ ).<sup>3</sup> At the  $\delta=0.5$  composition, these are present in equal numbers, forming alternating planes of  $\text{CoO}_5$  and  $\text{CoO}_6$  perpendicular to the  $c$  axis.<sup>1</sup>

The Co (III) ion in an octahedral environment as found in simple cobaltite perovskites such as  $\text{LaCoO}_3$  presents a challenging system, as the competition between the crystal field splitting and the intra-atomic exchange interaction is influenced by strong Co  $3d$ -O  $2p$  hybridization, affecting the on-site Coulomb repulsions.<sup>4</sup> The result is that three spin states for Co (III) are typically possible at temperatures in the range 100–400 K, the low spin state (LS) ( $t_{2g}^6 e_g^0$ ), the high spin state (HS) ( $t_{2g}^4 e_g^2$ ), and a state intermediate between these two (IS) ( $t_{2g}^5 e_g^1$ ).<sup>5</sup> The latter is thought to be stabilized by very strong Co  $3d$ -O  $2p$  hybridization, in effect existing as a mixture of  $t_{2g}^5 e_g^1$  and  $t_{2g}^5 e_g^2 \underline{L}^1$  states (where  $\underline{L}$  indicates a ligand hole).<sup>4</sup> For these systems, the Co exists in the LS state

at low temperatures (for  $\text{LaCoO}_3$ , below around 80 K), with transitions between LS and IS and between IS and HS as the temperature is raised. At high temperatures (in excess of 500 K for  $\text{LaCoO}_3$ ), the spin state is predominantly HS. There is increasing experimental data to suggest that the transitions between these three states occur gradually as a function of temperature, with an equilibrium population of all three at intermediate temperatures that shifts only slowly from majority LS to majority HS as the temperature is increased.<sup>5,6</sup>

One may anticipate similar spin state transitions at the octahedral  $\text{CoO}_6$  sites in the double perovskites, and indeed, this has been suggested to be the origin of the variations in magnetic susceptibility observed as a function of temperature in  $\text{GaBaCo}_2\text{O}_{5.5}$ .<sup>1</sup> The material undergoes a transition from antiferromagnetic (AFM) to ferromagnetic (FM) at around 220 K, and from ferromagnetic to paramagnetic at around 285 K.<sup>7</sup> In addition, the material shows changes in resistivity consistent with a nonmetal-to-metal transition at around 350 K.<sup>1,7</sup> However, there is currently considerable debate about the spin changes and orbital orderings giving rise to these transitions. Kim *et al.* conclude from magnetic susceptibility measurements that Co (III) in the octahedral sites of the structure is in the LS state only below 75 K, and is IS above this temperature.<sup>7</sup> The AFM to FM transition is then understood in terms of orbital ordering of the IS state  $e_g$  electron,<sup>7</sup> and the nonmetal-to-metal transition at around 350 K is understood in terms of the transition from IS to HS.<sup>7</sup> A similar origin for the nonmetal-to-metal transition in  $\text{TbBaCo}_2\text{O}_{5.5}$  is proposed by Moritomo *et al.*<sup>8</sup> In contrast, the Co ions at  $\text{CoO}_5$  pyramidal sites are believed to remain in the same spin

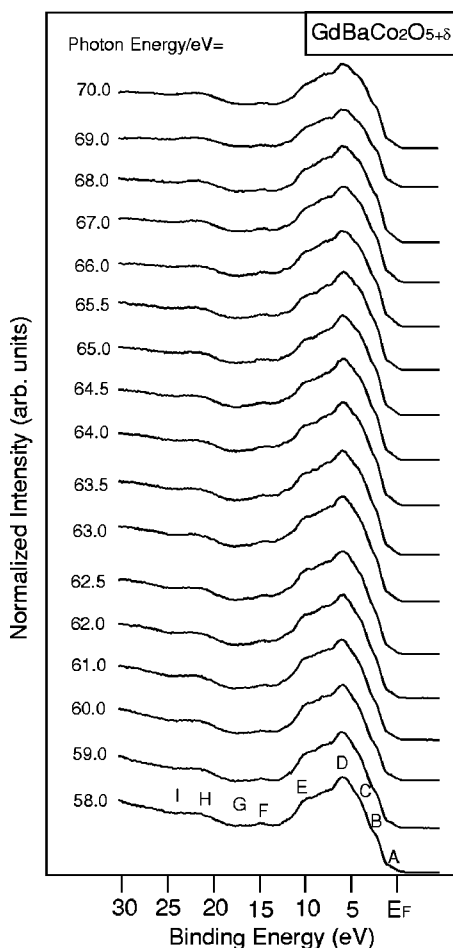


FIG. 1. Valence band EDCs recorded from  $\text{GdBaCo}_2\text{O}_{5+\delta}$  (001) in the vicinity of the Co  $3p \rightarrow 3d$  resonance at  $\sim 62$  eV photon energy. Points A–I refer to the points later selected for CIS measurements [Figs. 3(b) and 7]. The spectra are normalized to the incident photon flux.

state (IS) in the temperature regime where magnetic transitions are observed (typically 50–350 K).<sup>7</sup> The reduced symmetry of these pyramidal sites compared with the  $\text{CoO}_6$  octahedra lifts the degeneracy of the  $t_{2g}$  and  $e_g$  sites and lowers the crystal field (CF) stabilization, reducing the stability of the LS state compared with IS and HS. As a result, the LS state is not expected to be occupied even at very low temperature. While there appears to be some consensus of opinion that the spin state in the  $\text{CoO}_5$  pyramids does not change,<sup>1,7</sup> there are a number of different suggestions for the spin state variation with temperature in the octahedral sites. In contrast with Kim *et al.*<sup>7</sup> and Moritomo *et al.*,<sup>8</sup> Frontera *et al.*<sup>1</sup> attribute the nonmetal-to-metal transition at around 350 K to a sudden LS to HS transition in the octahedral sites. In marked disagreement, the LSDA+U calculations of Wu<sup>9–11</sup> suggest that the LS state in the double perovskites is less stable than in corresponding simple perovskites such as  $\text{LaCoO}_3$ . This author attributes both the AFM-FM and the nonmetal-to-metal transition to gradual  $pd\sigma$  hole delocalization in an “almost HS” state, implying that the HS state is predominant at much lower temperatures than in  $\text{LaCoO}_3$ .<sup>11</sup>

The determination of the Co (III) spin state in these materials, and the relationship of this to electronic structure is

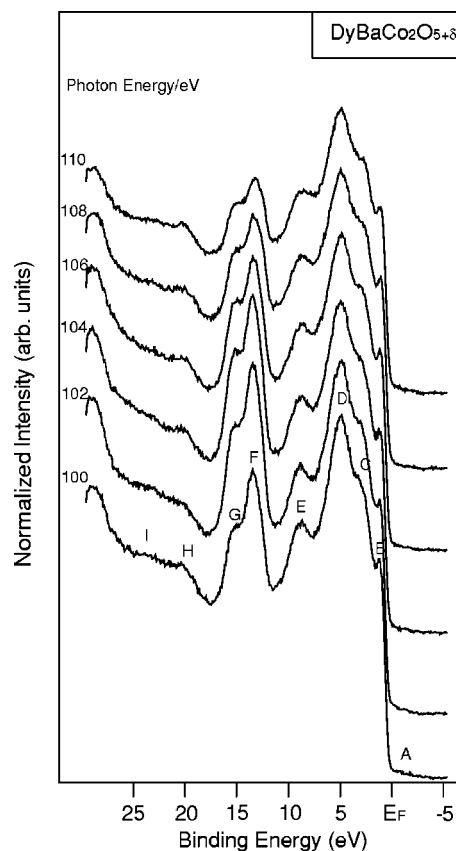


FIG. 2. Valence band EDCs recorded from  $\text{DyBaCo}_2\text{O}_{5+\delta}$  (001) in the vicinity of the Ba  $4d \rightarrow 4f$  resonance at  $\sim 104$  eV photon energy, illustrating the resonant enhancement of the Ba  $5p$  features at 14–16 eV BE (features F and G). Points A–I refer to the points later selected for CIS measurements [Figs. 4(b) and 7].

thus currently a topic of urgent investigation. Here we present valence band photoemission of single crystal  $\text{GdBaCo}_2\text{O}_{5+\delta}$  and  $\text{DyBaCo}_2\text{O}_{5+\delta}$ , concentrating on the use of resonant photoemission at the Co  $3p \rightarrow 3d$  and  $R 4d \rightarrow 4f$  thresholds to identify the atomic parentage of the valence band states. Co  $3p \rightarrow 3d$  resonance photoemission has previously been shown to be a powerful diagnostic of the LS (low spin) state of  $d^6$  Co (III) in cobaltites.<sup>12</sup> The resonance onset position of features associated with the LS state lies typically around 2.5 eV higher than those associated with Co (III) in HS (high spin) or IS (intermediate spin) states.<sup>12</sup> This is thought to be because the  $t_{2g}$  states are full in the LS state so the Co  $3p \rightarrow 3d$  transitions are delayed until the  $e_g$  states, which lie  $\sim 1$ –2 eV higher, can be occupied. Here we use this approach to confirm the presence of some IS/HS component of the Co (III) spin state in the double perovskites at temperatures as low as 50 K.

## EXPERIMENT

Single crystals of  $\text{GdBaCo}_2\text{O}_{5+\delta}$  and  $\text{DyBaCo}_2\text{O}_{5+\delta}$  of typical dimension  $2 \times 3 \times 2$  mm<sup>3</sup> were grown from an overstoichiometric flux melt. The oxygen content of the Gd crystal was determined from calibration curves relating the crystal lattice parameters (determined by x-ray diffraction) to

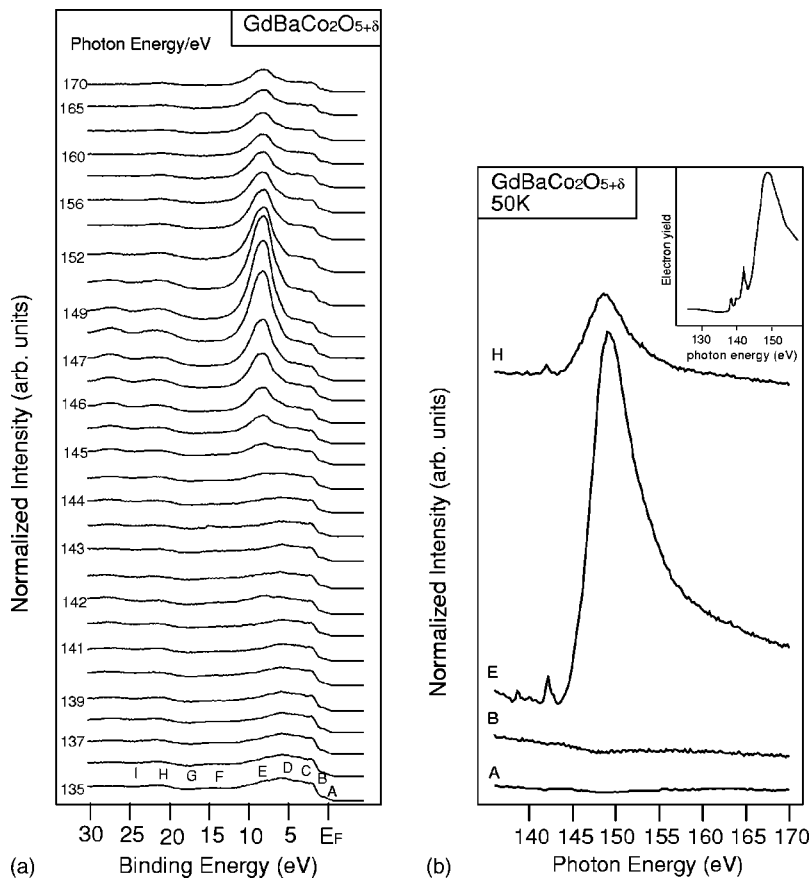


FIG. 3. (a) Valence band EDCs recorded from  $\text{GdBaCo}_2\text{O}_{5+\delta}$  (001) in the vicinity of the  $\text{Gd } 4d \rightarrow 4f$  resonance at  $\sim 150$  eV, illustrating the very large resonant enhancement of the valence band feature at 8 eV BE. Points A–I refer to the points selected for CIS measurements [Figs. 3(b) and 7]. The spectra were recorded at room temperature. (b) CIS spectra from  $\text{GdBaCo}_2\text{O}_{5+\delta}$  (001) in the region of the  $\text{Gd } 4d \rightarrow 4f$  resonance at selected points [labelled in Fig. 3(a)]. The spectra are normalized to the incident photon flux. The insert shows the photoelectron yield spectrum of Gd metal ( $4f^7$ ) recorded by Gerken *et al.* (Ref. 16) (see text). The spectra were recorded at 50 K.

oxygen content determined using iodometric titration.<sup>13</sup> This gave a value of  $\delta = 0.36 \pm 0.02$  for the Gd material, indicating a composition close to the completely Co (III) material  $\text{GdBaCo}_2\text{O}_{5.5}$ , but containing some reduced Co (II),  $d$ .<sup>7</sup> Temperature dependent magnetization measurements and magnetic hysteresis measurements for the  $\text{GdBaCo}_2\text{O}_{5+\delta}$  single crystal gave results strikingly similar to those presented by Kim *et al.*<sup>7</sup> for the  $\text{GdBaCo}_2\text{O}_{4.5}$  phase, but with a slightly broader ferromagnetic region. The onset of the paramagnetic-ferromagnetic transition was observed at around 290 K (cf. 280 K by Kim *et al.*<sup>7</sup>), while antiferromagnetic behavior was observed below 150 K (cf. 200 K by Kim *et al.*<sup>7</sup>). Laue backreflection from the largest faces showed clear diffraction patterns with the fourfold symmetry expected from the (001) face. The crystals were mounted with the large (001) faces parallel to the oxygen-free Cu sample plate using silver-loaded ultra high vacuum (UHV)-compatible epoxy (Ablestik). Clean surfaces of typically a few  $\text{mm}^2$  were prepared by fracturing with a clean diamond file in UHV at a pressure of better than  $5 \times 10^{-11}$  mbar. On subsequent examination, this was found to have fractured the surface giving a series of macroscopic steps parallel to the (001) plane. We regard the information obtained from these surfaces as effectively angle integrated. The cleaned sample surfaces were homogeneous, and typically stable over a period of 6–24 h in UHV. Sample cleanliness was checked by monitoring the evolution of contamination peaks at around 9.5 and 5.5 eV binding energy (BE) likely to be due to surface OH adsorption.<sup>12</sup> In general, the surfaces of the crystals were found to be more stable in UHV than those of simple

cobaltite perovskites such as  $\text{LaCoO}_3$ .<sup>12</sup> The sample was re-scraped as necessary, a process which reproducibly reestablished the clean surface. Rescraping within data sets was avoided.

Photoemission measurements were recorded on the multipole wiggler beamline MPW6.1 (PHOENIX, photon energy range  $40 \text{ eV} \leq h\nu \leq 350 \text{ eV}$ ) using the ARUPS 10 end station at the CLRC Daresbury laboratory SRS.<sup>14</sup> Energy distribution curves (EDC) were recorded with the sample at an angle of  $45^\circ$  to the incident photons and close to normal electron emission. Constant initial state (CIS) spectra were recorded in the same geometry with a fixed photon energy increment of 0.2 eV. All spectra are referenced to a Fermi edge recorded from the cleaned Cu sample plate and normalized to the  $I_0$  (flux) monitor of the beamline.  $I_0$  was recorded using a  $W$  mesh placed in the beamline just prior to the point where light enters the experimental chamber. The experimental (analyzer+beamline) resolution for valence band EDCs was 185 meV.

## RESULTS AND DISCUSSION

Figure 1 shows room temperature valence band photoemission spectra of  $\text{GdBaCo}_2\text{O}_{5+\delta}$  (001) taken at photon energies in the region of the  $\text{Co } 3p \rightarrow 3d$  resonance (at around 62 eV, and discussed later). The general features of the spectrum are a broad valence band (around 9 eV wide), with an additional small feature at around 15 eV BE. The valence band shows a small tail up to the Fermi energy, and the leading (low binding energy) edge shows features at around

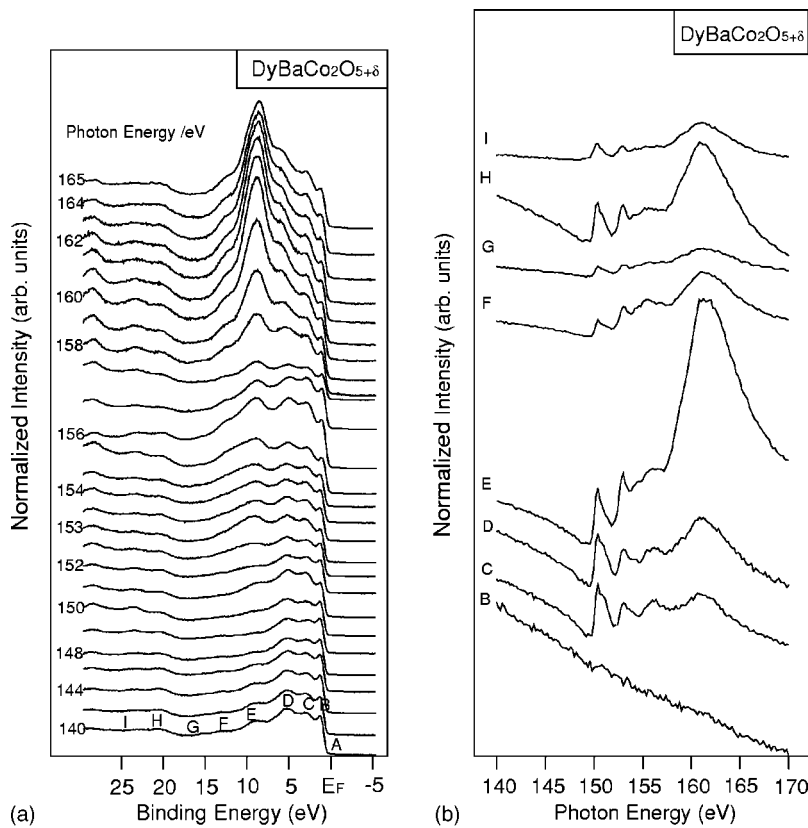


FIG. 4. (a) Valence band EDCs recorded from  $\text{DyBaCo}_2\text{O}_{5+\delta}$  (001) in the vicinity of the Dy  $4d \rightarrow 4f$  resonance at  $\sim 161$  eV, illustrating the very large resonant enhancement of the valence band feature at 9 eV BE. Points A–I refer to the points selected for CIS measurements [Fig. 4(b)]. (b) CIS spectra from  $\text{DyBaCo}_2\text{O}_{5+\delta}$  (001) in the region of the Dy  $4d \rightarrow 4f$  resonance at selected points [labelled in Fig. 4(a)]. The spectra are normalized to the incident photon flux. The spectra were recorded at room temperature.

2, 4, and 6 eV BE. Similar features are seen in the valence band spectrum of  $\text{DyBaCo}_2\text{O}_{5+\delta}$  as shown in Fig. 2 (taken at energies around the Ba  $4d \rightarrow 4f$  resonance, and discussed later). In the valence band region, we may reasonably expect contributions from Co  $3d$ , O  $2p$ , and R  $4f$  states; these contributions are explored by the resonant photoemission experiments described later. A distinct sharp feature at around 1–2 eV BE appears strongly in the spectra of simple perovskites such as  $\text{LaCoO}_3$ <sup>12,15,16</sup> and  $\text{HoCoO}_3$ ,<sup>17</sup> and has been associated with the presence of Co (III) in the LS state;<sup>15,16</sup> we note that this feature appears less pronounced in the case of the double perovskites.

In assigning the valence band features, we begin by identifying any contributions from Ba outside the valence band region. Figure 2 shows valence band spectra taken at energies in the vicinity of the Ba  $4d \rightarrow 4f$  resonance at  $\sim 104$  eV. This clearly identifies the Ba  $5p$  features in the region 14–16 eV BE (features F and G). The “giant” R  $4d \rightarrow 4f$  resonances for the Gd and Dy perovskites are explored in Figs. 3 and 4, respectively. These resonances, at around 150 eV photon energy and 162 eV photon energy, respectively, are so intense that they completely mask the underlying valence band [Figs. 3(a) and 4(a)] and are most conveniently displayed in CIS format as in Figs. 3(b) and 4(b). Figure 3(a) shows a very pronounced Gd resonance in the valence band at around 8 eV BE (feature E), which we assign to Gd  $4f$  states, and further small resonances at around 21 eV (feature H) and 27 eV BE, which we assign to Gd  $5p$  states (with spin-orbit splitting of approximately 6 eV). There appears to be no resonance of the low binding energy valence band states, indicating no appreciable  $4f$  contribution to these states. This is demonstrated more clearly in the CIS data of Fig. 3(b),

which have been normalized to the  $I_0$  reading so that an absolute comparison of intensities may be made. The resonance at 8 eV BE (feature E) is extremely pronounced, with a large broad feature centered at around 150 eV. The fine structure at around 138–144 eV is replicated in the smaller resonance observed at 21 eV BE (feature H), while there is no resonance in the low binding energy states close to the Fermi energy (1–2 eV binding energy, feature B).

The Gd  $4d \rightarrow 4f$  resonance has been a subject of extensive discussion in the literature since 1981.<sup>18–21</sup> For a general lanthanide configuration  $4f^n$ , the direct photoemission process may be described by electric dipole excitation of an  $f$  electron into continuum states  $\epsilon\ell$ :

$$4d^{10}4f^n \rightarrow 4d^{10}4f^{n-1} + \epsilon\ell.$$

Resonant photoemission is caused by a coherent superposition of this and the indirect channel opened up at resonance

$$4d^{10}4f^n \rightarrow 4d^9 4f^{n-1} \rightarrow 4d^{10}4f^{n-1} + \epsilon\ell,$$

i.e., creation of an intermediate  $4d$  hole state which decays through a radiationless super Coster-Kronig (sCK) Auger recombination to give the same final state as the direct process. The cross section enhancement is very effective at the  $4d \rightarrow 4f$  giant resonance, as both shells have the same principal quantum number and have similar radial distributions.

In Gd metal, which is a particularly simple case as the ground state is a half-filled shell ( $4f^7$ ), the  $4d \rightarrow 4f$  resonance consists of a broad and dominant absorption peak (the giant resonance), preceded by narrow and weak lines (the pre-edge region).<sup>18–21</sup> The narrow lines are believed to be due to forbidden “spin flip” transitions which occur during the reso-

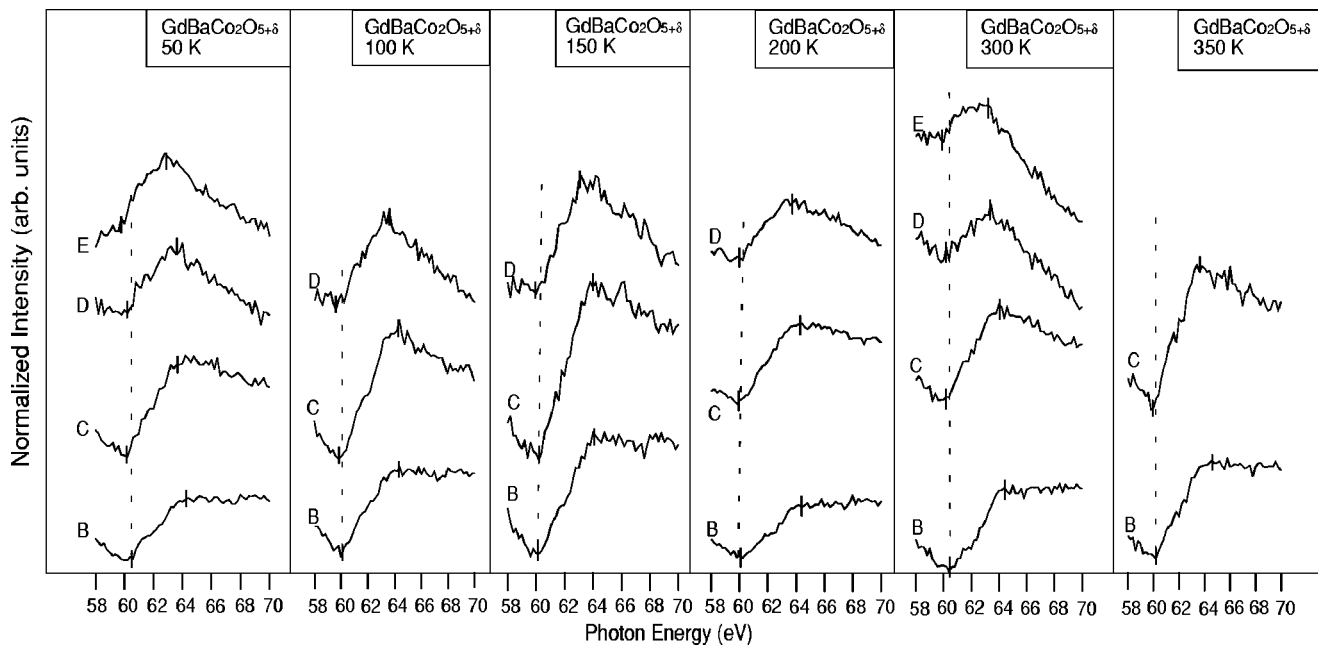


FIG. 5. CIS spectra at the Co  $3p \rightarrow 3d$  threshold recorded from  $\text{GdBaCo}_2\text{O}_{5+\delta}$  (001) as a function of temperature. Points B–E are defined in Fig. 3(a). The spectra are normalized to the incident photon flux.

nant photoemission process, although the stage of the process at which these occur (initial excitation or sCK decay) has been a subject of some controversy.<sup>21</sup> We note that both Gd metal and Gd (III) (the formal oxidation state anticipated here) are  $4f^7$  systems, so we expect strong similarities in resonant behavior; this is indeed the case, as can be seen by a comparison of the 8 eV BE resonance (feature E) with the photoelectron yield spectrum of Gd metal recorded by Gerken *et al.*<sup>18</sup> [inset, Fig. 3(b)].

In summary, the Gd resonance spectra confirm that the Gd ground state is  $4f^7$  in  $\text{GdBaCo}_2\text{O}_{5+\delta}$ , and show the  $4f$  contribution to the valence band density of states function to be centered at around 8 eV BE. Most importantly, there is no  $4f$  contribution within several electron volts of the Fermi energy, and we thus anticipate that these states have entirely Co  $3d$  and O  $2p$  character. Generally similar features are observed for  $\text{DyBaCo}_2\text{O}_{5+\delta}$  at the Dy  $4d \rightarrow 4f$  resonance, shown in Figs. 4(a) and 4(b). Here the ground state [assuming a Dy (III) oxidation state in the double perovskite] is  $4f^9$ . This resonance is less well-studied than in the Gd case,<sup>22</sup> but as the ground state is no longer half-filled, a more complex resonance signal is anticipated, as seen in the CIS spectra of Fig. 4(b). The  $4f$  contribution to the valence band is seen to be centered at around 9 eV BE [feature E, Fig. 4(b)], with  $5p$  contributions in the range 20–27 eV BE. Again, no resonance is observed for features close to the Fermi energy [e.g., the feature at 1 eV BE, feature B, Fig. 4(b)], showing that the states near  $E_f$  have no  $4f$  character. The Co  $3d$  character of these states is probed by experiments at the Co  $3p \rightarrow 3d$  resonance described later.

Resonant effects at transition metal  $3p \rightarrow 3d$  thresholds are seen for a wide range of materials, albeit with much smaller cross sections than the giant  $R 4d \rightarrow 4f$  resonances. The processes occurring for the Co (III) initial state configuration are given later. The direct photoemission process may be written

$$3p^6 3d^6 + h\nu \rightarrow 3p^6 3d^5 + \varepsilon \ell.$$

At photon energies larger than the  $3p \rightarrow 3d$  absorption threshold, the direct process is supplemented by initial  $3p \rightarrow 3d$  excitation, followed by super Coster-Kronig Auger decay

$$3p^6 3d^n + h\nu \rightarrow 3p^5 3d^7 \rightarrow 3p^6 3d^6 + \varepsilon \ell.$$

We may therefore expect the observed binding energy of the resonance features to be affected by the initial occupancy of the  $d$  orbitals, and the resonance position may therefore reflect the spin state of the sample.<sup>12</sup>

The low cross section of the Co  $3p \rightarrow 3d$  resonance has the result that the spectral changes in the region of the resonance are scarcely discernible in valence band EDCs (Fig. 1), and CIS mode is required to reveal them. Figure 5 shows CIS spectra recorded over the Co  $3p \rightarrow 3d$  resonance for  $\text{GdBaCo}_2\text{O}_{5+\delta}$  as a function of temperature. The spectra have been normalized to the  $I_0$  reading so that an absolute comparison of intensities may be made. The binding energy positions chosen for the CIS spectra are labelled in Fig. 1. For comparison, analogous data for a simple perovskite,  $\text{LaCoO}_3$  are also shown in Fig. 6.<sup>23</sup> It can be seen from Fig. 5 that in the case of  $\text{GdBaCo}_2\text{O}_{5+\delta}$  the Co  $3p \rightarrow 3d$  resonance is a weak, broad feature centered at around 62 eV photon energy, with a resonance onset typically around 60.5 eV, rising to a maximum at around 64 eV. Some evidence of a Co resonance is seen for all the valence band energies chosen, indicating that the Co  $3d$  states are widely spread throughout the valence band. Of particular interest is the resonance behavior of the valence band feature at around 2 eV BE (feature B), which in simple perovskites has been associated predominantly with the presence of Co (III) in the LS state.<sup>12,15,16</sup> This is shown in more detail for both  $\text{GdBaCo}_2\text{O}_{5+\delta}$  and  $\text{DyBaCo}_2\text{O}_{5+\delta}$  in Fig. 7. This feature shows a resonance on-

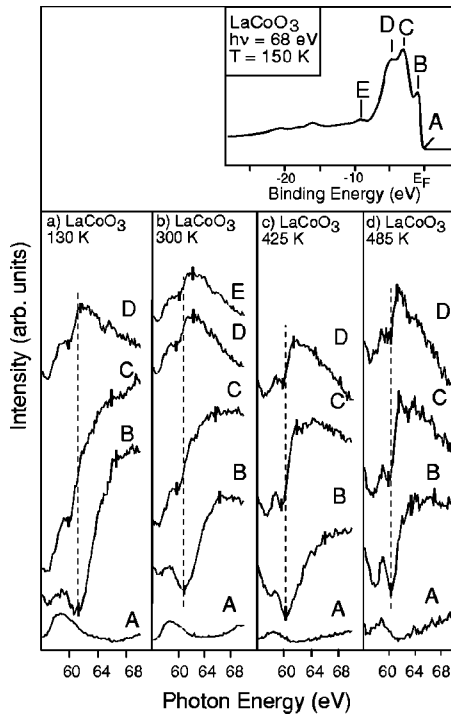


FIG. 6. CIS spectra at the Co  $3p \rightarrow 3d$  threshold recorded from  $\text{LaCoO}_3$  (111) as a function of temperature. Points A–E refer to the valence band positions marked on the inset EDC spectrum. The dashed lines originating at the resonance minimum of feature B are drawn to emphasise the  $\sim 2$  eV shift in resonance onset position between features B and C–E at low temperature. Spectra are normalized to the incident photon flux. The small feature observed at 59 eV at point A is not an intrinsic part of the resonance (Ref. 12). Adapted from Ref. 12.

set at around 60.5 eV which is invariant with temperature down to the lowest temperature probed (50 K for  $\text{GdBaCo}_2\text{O}_{5+\delta}$  and 100 K for  $\text{DyBaCo}_2\text{O}_{5+\delta}$ ), and which is similar to the onset energy of the other valence band resonances probed (Fig. 5). There appear to be no large changes in intensity of this resonance relative to the other valence band resonances as a function of temperature (Fig. 5).

This unexceptional behavior is in marked contrast with the behavior of simple perovskites, such as  $\text{LaCoO}_3$ <sup>12</sup> (Fig. 6) and  $\text{HoCoO}_3$ .<sup>17</sup> The first obvious experimental difference is that in the case of the double perovskites, it is possible to record data without sample charging to temperatures as low as at least 50 K, whereas in the case of  $\text{LaCoO}_3$ , severe charging is encountered below 130 K<sup>12</sup> (accounting for the truncated temperature range in Fig. 6). This indicates that the double perovskites have appreciable low temperature conductivity, which is not consistent with the majority of Co in the sample entering the LS (nonconducting state) at low temperature as in the simple perovskites. In the case of simple perovskites such as  $\text{LaCoO}_3$  (Fig. 6) it is clear that the resonance onsets for the “2 eV BE” feature (feature B) at low and room temperature are at higher energy than for the other features, an effect clearly absent in the case of the double perovskites (Fig. 5). As most of the intensity of this resonance in the simple perovskite at low temperature derives from LS Co (III),<sup>15,16</sup> this is expected. In the low spin state

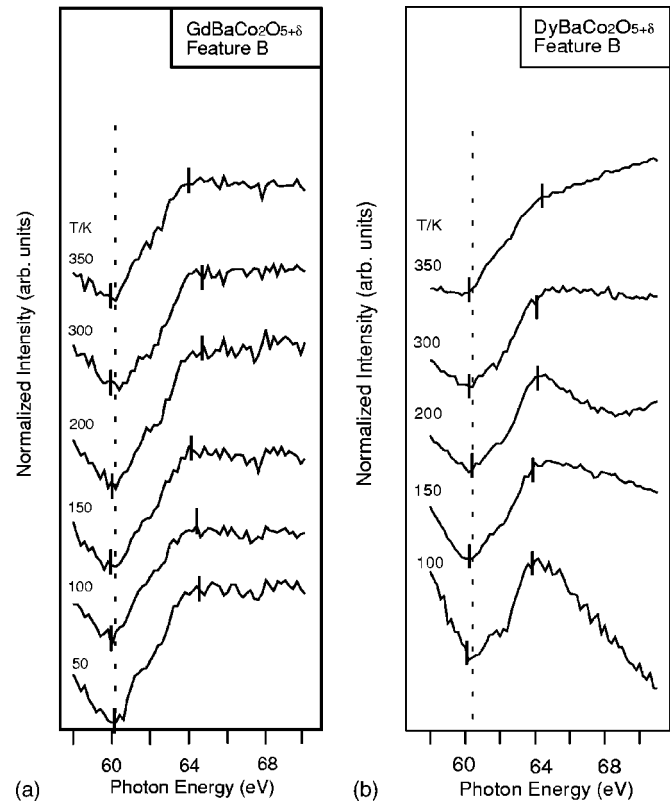


FIG. 7. Temperature variation of the CIS spectra at the Co  $3p \rightarrow 3d$  threshold for the 2 eV BE feature [point B in Figs. 1, 2, 3(a), and 4(a)] of (a)  $\text{GdBaCo}_2\text{O}_{5+\delta}$  (001) and (b)  $\text{DyBaCo}_2\text{O}_{5+\delta}$  (001). The data are normalized to the incident photon flux.

all of the  $t_{2g}$  states are full, so only the  $e_g$  states (which according to calculations lie approximately 1.1–2 eV above the  $t_{2g}$  states)<sup>4,24,25</sup> can contribute to the spectrum leading to a delayed resonance onset. In the higher binding energy parts of the valence band which correspond to Co in intermediate ( $t_{2g}^5 e_g^1$  and  $t_{2g}^5 e_g^2 \underline{L}$ , where  $\underline{L}$  represents a ligand hole), and high spin ( $t_{2g}^4 e_g^2$ ) states we now have empty  $t_{2g}$  states for the Co  $3p$  electrons to be excited into, thus the resonance onset is at a lower energy at these points. The observation of this delayed resonance has been used as a diagnostic of the Co (III) LS state in simple perovskites.<sup>12</sup> As the temperature is raised, and the low spin state is depopulated in favor of IS and HS, it can be seen from Fig. 6 that the delayed resonance effect disappears (all resonance onsets are aligned at 485 K), and further, the intensity of the resonance at 2 eV BE (feature B) is reduced relative to the other valence band resonances. In sharp contrast, for  $\text{GdBaCo}_2\text{O}_{5+\delta}$  and  $\text{DyBaCo}_2\text{O}_{5+\delta}$  (Fig. 7), the resonance onset of feature B is undelayed at all temperatures down to 50 K for  $\text{GdBaCo}_2\text{O}_{5+\delta}$  and 100 K for  $\text{DyBaCo}_2\text{O}_{5+\delta}$ , occurring at the same energy as the onsets of the other valence band resonances ( $\sim 60.5$  eV). This demonstrates that even at the lowest temperatures probed, a significant proportion of the Co (III) in the double perovskites is not in the LS state. This is consistent with the idea that the Co (III) in pyramidal sites remains in an unchanged (probably IS) state at all temperatures.<sup>7</sup> Because of the presence of the undelayed resonance in all the spectra, it is difficult to find evidence for LS Co (III) in the CIS data. The only pos-

sible indication of the presence of the LS state is that for both double perovskites, the lowest temperature spectrum in Fig. 7 appears to show a “double rise,” with an initial onset at 60.5 eV and a second onset at around 63 eV; this is most evident in the case of  $\text{DyBaCo}_2\text{O}_{5+\delta}$  [Fig. 7(b)]. This double feature is apparently reduced in intensity as the temperature of the  $\text{DyBaCo}_2\text{O}_{5+\delta}$  sample is raised, and is lost by 350 K. This may suggest some occupation of the LS state at low temperature that is progressively lowered as the temperature is raised. However, the changes in the  $\text{GdBaCo}_2\text{O}_{5+\delta}$  spectra [Fig. 7(a)] are far less clear, and these data do not allow us to infer the presence of LS Co (III).

Definitive evidence for a significant change in the proportion of LS Co (III) is similarly difficult to extract from valence band EDCs taken as a function of temperature. As previously noted, the 2 eV BE feature (feature B) appears to be much less pronounced in the case of double perovskites than in the spectra of simple perovskites such as  $\text{LaCoO}_3$ <sup>12,15,16</sup> and  $\text{HoCoO}_3$ .<sup>17</sup> In the latter cases, a distinct sharp feature at 1–2 eV BE appears strongly in the spectra at low temperatures, and decreases in intensity as the sample temperature is raised<sup>12,15,17</sup> (Fig. 6, inset). This feature has been associated with Co (III) in the LS state (more specifically to a transition of  ${}^2T_2$  symmetry corresponding to the  $t_{2g}^6 ({}^1A_1) + h\nu \rightarrow t_{2g}^5 ({}^2T_2) + e$  photoemission channel).<sup>15,16</sup> As this association has been made largely through configuration interaction calculations using octahedral  $\text{CoO}_6^{9-}$  clusters,<sup>16</sup> we expect to observe a similar feature in the valence band EDCs of any system containing LS Co (III) in an octahedral environment. Although a feature at 2 eV BE is present in the spectra of the double perovskites, it is not resolved from the main valence band, and appears to show no variation in intensity over the whole of the temperature range (50–400 K) studied here. (In fact, the only marked changes we observed in the spectra as a function of temperature could be associated with surface degradation, particularly at low temperatures.) An example is shown in Fig. 8, where normalized spectra taken in the range of the 2 eV feature (feature B) of  $\text{GdBaCo}_2\text{O}_{5+\delta}$  over the temperature range 300–400 K are shown. This temperature range is of particular interest, as changes in resistivity,<sup>3</sup> lattice parameters,<sup>1</sup> and susceptibility,<sup>1</sup> which have been associated with a metal-to-nonmetal transition, have been observed at around 350 K for  $\text{GdBaCo}_2\text{O}_{5+\delta}$ . If the metal-to-nonmetal transition is associated with a sharp HS-LS transition in the octahedral sites, as has been suggested,<sup>1</sup> then we would expect to observe very marked changes in the intensity of the 2 eV feature associated with LS in this range, and a loss of the density of states at the Fermi energy. In fact, as can be seen in Fig. 8, no significant changes in any of the spectral features are observed in this temperature range. We cannot rule out the possibility that the absence of the transition in our spectra may be simply due to the fact that the oxygen content of our crystal ( $\delta=0.36$ ) is slightly different from the ideal “all Co (III)” composition,  $\delta=0.5$ , so that the crystal will contain some reduced Co (II),  $d^7$ , with around one in ten cobalt ions having a  $t_{2g}^6 e_g^1$  configuration. This, combined with the strong hysteresis in the metal-to-nonmetal transition temperature recently reported by Doroshev *et al.*,<sup>26</sup> means that the transition may lie outside the range of investigation. However, the

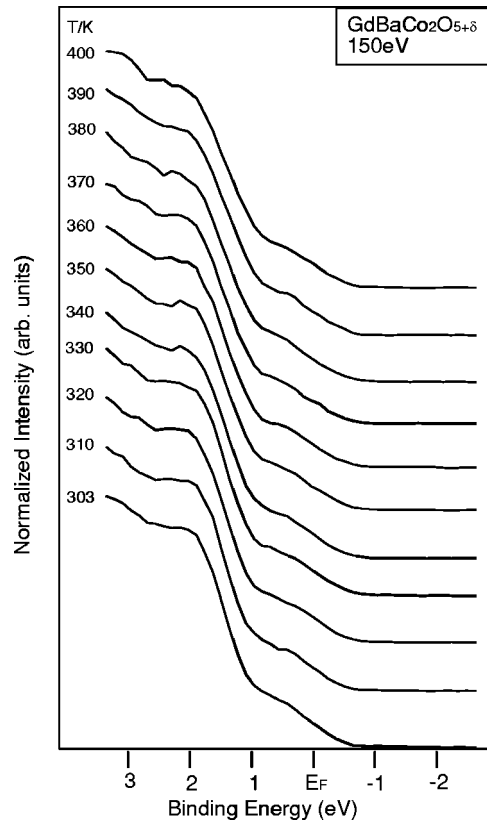


FIG. 8. Valence band EDCs recorded from  $\text{GdBaCo}_2\text{O}_{5+\delta}$  (001) in the vicinity of the Fermi energy in the temperature range 300–400 K. The data are normalized to the incident photon flux.

absence of any variation in intensity in the “Co LS peak” at 2 eV BE (feature B) militates against a rapid LS-HS spin flip in the octahedral sites in this temperature range.

This general conclusion appears to be supported by available band structure calculations for the double perovskites, although there are also significant discrepancies between our experiment and these calculations. Figure 9 shows a comparison between the valence band spectrum for  $\text{GdBaCo}_2\text{O}_{5+\delta}$  at 300 K and LSDA+U calculations by Wu<sup>11</sup> for a hypothetical FM state at 300 K. Some caution needs to be exercised in comparing our one electron removal spectra with a ground state calculation. In addition, the appearance of the experimental spectra is weighted by the difference in the photoionization cross-sections of the Co  $3d$  and O  $2p$  states. For the purposes of the comparison in Fig. 8 we have chosen a photon energy of 58 eV, where the O  $2p$  and Co  $3d$  cross sections are relatively similar ( $\sigma_{\text{O}:2p}/\sigma_{\text{Co}:3d} = 6 \text{ Mb atom}^{-1}/8.5 \text{ Mb atom}^{-1}$ ).<sup>27</sup> The calculations show a valence band of around 8 eV wide, composed of Co  $3d$  and O  $2p$  states, broadly in agreement with experiment. Gd  $4f$  states are not included in the calculation as valence states; in our experiment, we showed these to be located around 8 eV BE, with no detectable contribution at lower binding energy.

From the calculated data one can infer the spin state from the filling of the majority and minority spin states (indicated in full and dashed lines, respectively). In the case of an HS state, the majority spin channel is completely filled, whereas for a LS state, the  $e_g$  states for both majority and minority channels should be completely empty. As can be seen from

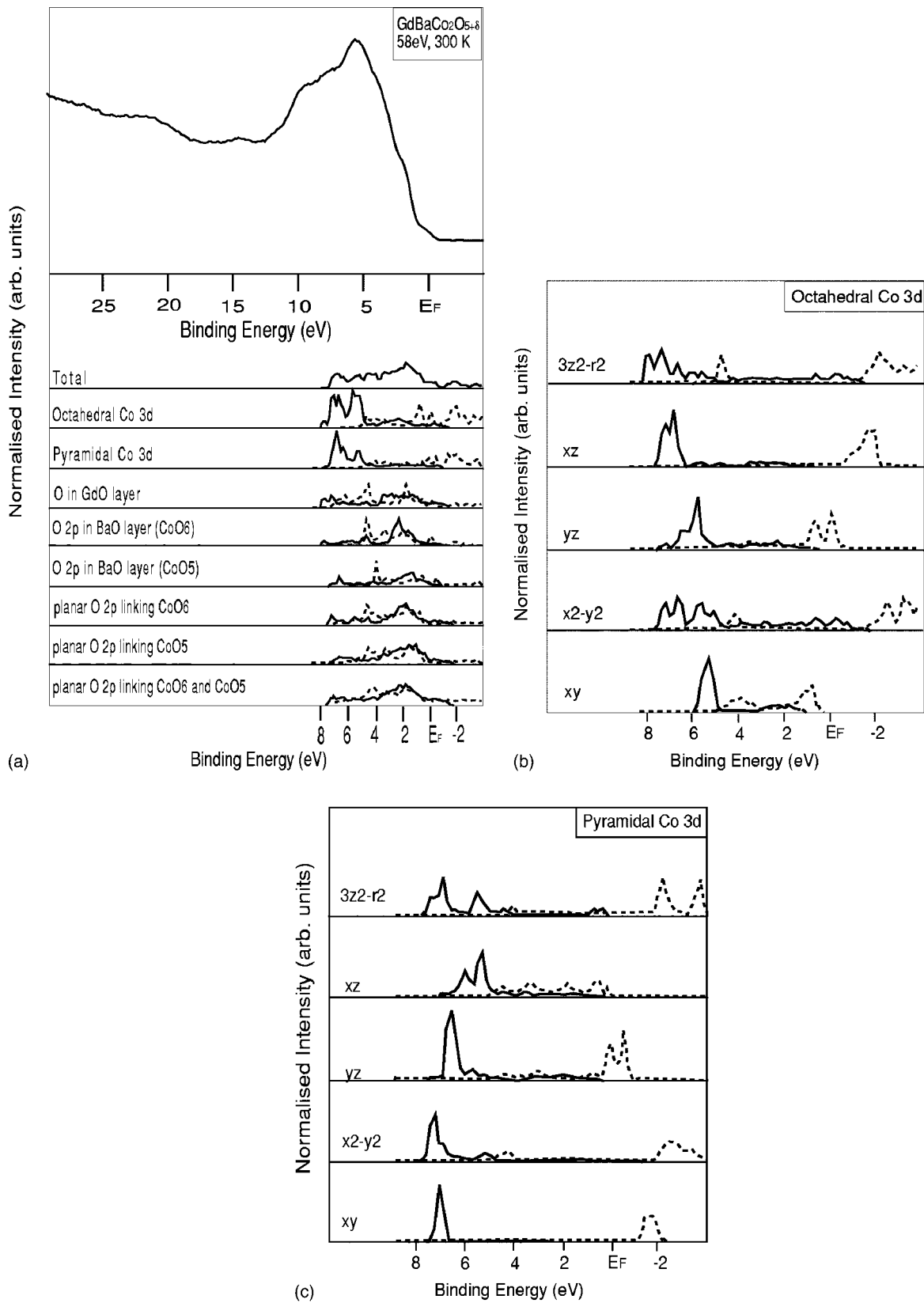


FIG. 9. (a) Comparison of the experimental EDC of  $\text{GdBaCo}_2\text{O}_{5+\delta}(001)$  recorded at 58 eV photon energy and 300 K with the bulk band structure calculations of Wu (Ref. 11) for a hypothetical ferromagnetic phase at 300 K. The calculations have been aligned with experiment at the Fermi energy. In the calculation solid and dotted lines represent majority and minority spin states, respectively. (b)  $d$  orbital contributions to the calculated density of states function for pyramidal and octahedral Co(III), adapted from Ref. 11. Solid and dotted lines represent majority and minority spin states, respectively.



Fig. 9(b), the spin state predicted by the calculation in the octahedral sites is very close to HS for the FM phase [(similarly the calculation for the antiferromagnetic phase (AFM) expected at lower temperature (not shown) also somewhat surprisingly shows an almost HS state)]. The Co in the pyramidal sites is taken to be in a localized HS state from the calculation.<sup>11</sup> Both the AFM/FM and nonmetal-to-metal transitions in this calculation occur through gradual delocalization of the  $pd\sigma$  holes in the almost HS state of  $\text{GdBaCo}_2\text{O}_{5.5}$ ,<sup>11</sup> rather than through a sudden Co LS-HS spin flip. Overall the calculation suggests that the HS state is much more stable in double perovskites such as  $\text{GdBaCo}_2\text{O}_{5+\delta}$  than in simple perovskites such as  $\text{LaCoO}_3$ . This is attributed to two effects. The first is a smaller calculated splitting in the double perovskite (1.0 eV for  $\text{GdBaCo}_2\text{O}_{5.5}$  vs 1.2 eV in  $\text{LaCoO}_3$ ),<sup>11</sup> an effect that makes the LS state less stable in the double perovskite. This is coupled with weaker  $pd\sigma$  hybridization in the double perovskite, due to strong corrugation of the “ $\text{CoO}_4$ ” basal plane of the octahedra. Strong  $pd\sigma$  hybridization stabilizes the IS state relative to LS and IS in  $\text{SrCoO}_3$ <sup>28</sup> and  $\text{La}_{1-x}\text{Sr}_x\text{CoO}_3$ .<sup>4,16</sup> Thus overall, both LS and IS states are expected to be less stable in double perovskites than in simple perovskites.<sup>11</sup> The predicted lower stability of the LS state correlates well with our experimental observations that the LS state is much less obvious in the spectra (either the CIS or the EDC data) at a given temperature than for simple perovskites such as  $\text{LaCoO}_3$ <sup>12,15,16</sup> or  $\text{HoCoO}_3$ .<sup>17</sup> However, we stress that our experiments are a particularly sensitive diagnostic of the LS state only; we are unable to distinguish effectively between HS and IS states. Thus, while our experiments suggest that a rapid HS-LS spin flip at the metal-to-nonmetal transition is unlikely, we are unable to distinguish between the HS-HS “delocalization” model of Wu *et al.*,<sup>11</sup> and the IS-HS mechanism proposed by Kim *et al.*<sup>7</sup> and Moritomo *et al.*<sup>8</sup>

The absence of any dramatic changes in the spectra as a function of temperature also suggests that the electronic structure changes giving rise to changes in magnetic behavior are gradual and subtle. This is in contrast with the results of other measurements (particularly diffraction) which suggest rapid changes in the vicinity of the phase transition.<sup>1</sup> A similar apparent contradiction is observed in the simple perovskites, notably  $\text{LaCoO}_3$ , where photoemission shows a gradual evolution from a mostly LS state at low temperature, to a mostly HS state at high temperature, via an IS state.<sup>12,15</sup> Indeed, the photoemission data may be fitted to the three-state model of Asai *et al.*,<sup>12</sup> where a shifting equilibrium between different proportions of LS, IS, and HS states exists at all temperatures.<sup>5</sup> In contrast, bulk susceptibility and lattice parameter measurements for  $\text{LaCoO}_3$  show sudden changes with temperature<sup>6,29</sup> which were again initially interpreted in terms of a simple and sudden LS-HS transition in the  $\text{CoO}_6$  octahedra,<sup>30</sup> but were later shown to be consistent with a three-state model.<sup>6</sup> Similarly, our photoemission data for the double perovskites indicate that the mechanism for the phase transition is more subtle than a sudden LS-HS switch.

The calculation for the FM phase shows a low density of states (DOS) at the Fermi energy ( $E_F$ ), arising from weakly delocalized minority spin Co  $d_{yz}$  orbitals in both octahedral

and pyramidal sites. A small DOS at  $E_F$  is observed experimentally (Figs. 8 and 9). However, the observation of this DOS in our experiment at room temperature (below the anticipated nonmetal-to-metal transition) is unexpected, as discussed earlier. The calculation also shows the main Co  $3d$  contributions to the valence band to lie around 1 and 6–8 eV below the Fermi energy, with the filled states between these energies having mostly O  $2p$  character (from O in the basal plane, and at the apices both in the Gd layers and the Ba layers of the structure). In contrast, our resonant photoemission taken at the Co  $3p$ - $3d$  threshold (Fig. 5) shows no strong variation in the intensity of the Co  $3p$ - $3d$  resonance and thus in the Co  $3d$  character across the valence band. In particular, we do not observe an enhancement in the resonance intensity at 6–8 eV binding energy. This means that the Co  $3d$ -O  $2p$  hybridization of the valence band states observed experimentally is stronger than predicted by the calculation. This is a factor that will make the IS state more stable relative to LS and HS than suggested from the calculation.

## CONCLUSIONS

Resonant photoemission measurements from single crystal (001) surfaces of the double perovskites  $\text{GdBaCo}_2\text{O}_{5+\delta}$  and  $\text{DyBaCo}_2\text{O}_{5+\delta}$  indicate that the valence band is made up of strongly hybridized O  $2p$  and Co  $3d$  states. The Gd and Dy  $4f$  contributions to the valence band are centered at around 8 eV BE for Gd and around 9 eV BE for Dy. In both cases there are no  $4f$  states close to the Fermi energy, and the Gd  $4d$ - $4f$  resonance confirms a Gd (III) oxidation state. The valence band electronic structure contrasts markedly with that observed for simple perovskites such as  $\text{LaCoO}_3$ <sup>12,15,16</sup> and  $\text{HoCoO}_3$ <sup>17</sup> in that no marked intensity variations are observed with temperature in the range 50–400 K. The valence band feature at around 2 eV BE [associated with LS Co (III) in the case of simple perovskites] is less pronounced than in the cases of  $\text{LaCoO}_3$  and  $\text{HoCoO}_3$ , and, unlike the simple perovskites, shows no strong intensity variation with temperature. This strongly suggests that the phase transition observed in this material at around 350 K is not associated with a sudden LS-HS spin switch in the octahedral sites.<sup>1</sup> The associated metal-to-nonmetal transition was not observed as a change in the DOS at  $E_F$ , which showed the characteristics of a poor metal in the range 300–400 K. The reasons for this are unclear, but may be associated with the presence of  $d^7$  Co (II) cations in the sample. Co  $3p$ - $3d$  resonance photoemission shows an undelayed onset at temperatures as low as 50 K, indicating that some Co remains in an IS or HS state in the sample at very low temperatures. This accords with the idea that the Co spin state in the pyramidal sites of the material is unchanged with temperature. At the lowest temperatures studied, some slight possible evidence of a second “delayed” resonance, characteristic of Co (III) in an LS state,<sup>12</sup> is observed, which has disappeared by 350 K.

The subtle and gradual changes in the CIS data with temperature, and the absence of marked temperature variations in the EDCs suggest that any spin changes in these materials are similarly gradual. The lack of a strong photoemission

feature due to LS Co (III) in the valence band EDCs suggests that the LS state is less stable in these materials than in a simple Co (III) perovskite at the same temperature. This finding is in agreement with LSDA+U band structure calculations for  $\text{RBaCo}_2\text{O}_{5.5}$ ,<sup>9–11</sup> where the effect is attributed to the smaller CF splitting in the double perovskite.<sup>11</sup> However, Co  $3p$ - $3d$  resonant photoemission indicates stronger O  $2p$ -Co  $3d$  hybridization than predicted by the calculation, and this will stabilize the IS state relative to the prediction of the calculation.<sup>4,16,28</sup> In our experiments we are unable to distinguish between IS and HS states, so we are unable to comment on the hypothesis of Wu that the spin state in the AFM and FM phases is close to HS.<sup>11</sup> Similarly, in the case of the metal-to-nonmetal transition, although our data indicate that the mechanism is more subtle than a sudden LS-HS switch,<sup>1</sup> we are unable to distinguish between the HS-HS delocalization model of Wu *et al.*<sup>11</sup> and the IS-HS mecha-

nism proposed by Kim *et al.*<sup>7</sup> and Moritomo *et al.*<sup>8</sup> Nevertheless, our experiments indicate that the spin equilibrium in the double perovskites is significantly shifted in favor of higher spin multiplicities compared with materials such as  $\text{LaCoO}_3$ <sup>12,15,16</sup> and  $\text{HoCoO}_3$ .<sup>17</sup>

#### ACKNOWLEDGMENTS

This work was supported under INTAS Grant No. 01-0278. The authors thank Dr. Andrei Podlesnyak of PSI Villigen, Dr. Robin Pritchard of the Chemistry Department at UMIST, and Dr. Peter Mitchell of the Schuster Laboratory, University of Manchester, for assistance in characterizing the single crystals used in this work. R.J.S., R.L.K., and P.T.S. were supported by Louisiana State University. D.T. is supported by EPSRC (UK) and CCLRC (UK).

\*Author to whom correspondence should be addressed. Electronic address: wendy.flavell@manchester.ac.uk

<sup>1</sup>E.g., C. Frontera, J. L. Garcia-Munoz, A. Llobet, and M. A. G. Aranda, *Phys. Rev. B* **65**, 180405 (2002).

<sup>2</sup>A. Ducouret, J. M. Greneche, and B. Raveau, *J. Solid State Chem.* **114**, 24 (1995).

<sup>3</sup>A. Maignan, C. Martin, D. Pelloquin, N. Nguyen, and B. Raveau, *J. Solid State Chem.* **142**, 247 (1999).

<sup>4</sup>M. A. Korotin, S. Yu. Ezhov, I. V. Solovyev, V. I. Anisimov, D. I. Khomskii, and G. A. Sawatzky, *Phys. Rev. B* **54**, 5309 (1996).

<sup>5</sup>K. Asai, A. Koned, O. Yokokura, J. M. Tranquada, G. Shirane, and K. Kohn, *J. Phys. Soc. Jpn.* **67**, 290 (1998).

<sup>6</sup>P. G. Radaelli and S.-W. Cheong, *Phys. Rev. B* **66**, 094408 (2002).

<sup>7</sup>W. S. Kim, E. O. Chi, H. S. Choi, N. H. Hur, S.-J. Oh, and H.-C. Ri, *Solid State Commun.* **116**, 609 (2000).

<sup>8</sup>Y. Moritomo, T. Akimoto, M. Takeo, A. Machida, E. Nishibori, M. Takata, M. Sakata, K. Ohoyama, and A. Nakamura, *Phys. Rev. B* **61**, R13325 (2000).

<sup>9</sup>H. Wu, *Phys. Rev. B* **64**, 092413 (2001).

<sup>10</sup>H. Wu, *Phys. Rev. B* **62**, R11953 (2000).

<sup>11</sup>H. Wu, *J. Phys.: Condens. Matter* **15**, 503 (2003).

<sup>12</sup>A. G. Thomas, W. R. Flavell, P. M. Dunwoody, C. E. J. Mitchell, S. Warren, S. C. Grice, P. G. D. Marr, D. E. Jewitt, N. Khan, S. W. Downes, D. Teehan, E. A. Seddon, K. Asai, Y. Koboyashi, and N. Yamada, *J. Phys.: Condens. Matter* **12**, 9259 (2000).

<sup>13</sup>A. Podlesnyak (private communication).

<sup>14</sup>M. Bowler, J. B. West, F. M. Quinn, D. M. P. Holland, B. Fell, P. A. Hatherly, I. Humphrey, W. R. Flavell, and B. Hamilton, *Surf. Rev. Lett.* **9**, 577 (2002).

<sup>15</sup>M. Abbate, J. C. Fuggle, A. Fujimori, L. H. Tjeng, C. T. Chen, R. Potze, G. A. Sawatzky, H. Eisaki, and S. Uchida, *Phys. Rev. B* **47**, 16124 (1993).

<sup>16</sup>T. Saitoh, T. Mizokawa, A. Fujimori, M. Abbate, Y. Takeda, and M. Takano, *Phys. Rev. B* **55**, 4257 (1997).

<sup>17</sup>W. R. Flavell, A. G. Thomas, D. Tsoutsou, A. K. Mallick, E. A. Seddon, C. Cacho, A. E. R. Malins, R. L. Stockbauer, R. L. Kurtz, P. T. Sprunger, S. N. Barilo, S. V. Shiryaev, and G. L. Bychkov (unpublished).

<sup>18</sup>F. Gerken, J. Barth, and C. Kunz, *Phys. Rev. Lett.* **47**, 993 (1981).

<sup>19</sup>T. Kachel, R. Rochow, W. Gudat, R. Jungblut, O. Rader, and C. Carbone, *Phys. Rev. B* **45**, 7267 (1992).

<sup>20</sup>K. Starke, E. Navas, E. Arenholz, Z. Hu, L. Baumgarten, G. van der Laan, C. T. Chen, and G. Kaindl, *Phys. Rev. B* **55**, 2672 (1997).

<sup>21</sup>Z. Hu, K. Starke, G. van der Laan, E. Navas, A. Bauer, E. We-  
schke, C. Schüssler-Langeheine, E. Arenholz, A. Mühlig, G. Kaindl, J. B. Goodkoop, and N. B. Brookes, *Phys. Rev. B* **59**, 9737 (1999).

<sup>22</sup>E.g., G. van der Laan and B. T. Thole, *Phys. Rev. B* **48**, 210 (1993).

<sup>23</sup>Adapted from Ref. 12.

<sup>24</sup>S. Yamaguchi, Y. Okimoto, and Y. Tokura, *Phys. Rev. B* **54**, R11022 (1996).

<sup>25</sup>The total drop in energy of the midpoint of the resonance (defined as the midpoint between the tic marks shown in Fig. 6 over the range 130–500 K measured in Ref. 12 is approximately 2 eV, which approximately corresponds to the crystal field stabilization energy. It should be noted that there will also be a contribution from the energy differences in electron correlation and charge transfer effects, depending on the electronic configuration changes occurring between the different spin states (i.e., to account for the fact that in the region of LS the CIS experiment excites an electron into the empty  $e_g$  state, whereas in the IS case an electron is excited into a  $t_{2g}$  state already containing five electrons and the  $e_g$  also contains one or two electrons), thus the measured energy difference we measure here will not be purely the crystal field splitting (10 Dq).

<sup>26</sup>V. D. Doroshev, V. A. Borodin, Yu. G. Pashkevich, V. I. Kame-  
nev, A. S. Mazur, and T. N. Tarasenko (unpublished).

<sup>27</sup>J. J. Yeh and I. Lindau, *At. Data Nucl. Data Tables* **32**, 1 (1985).

<sup>28</sup>R. H. Potze, G. A. Sawatzky, and M. Abbate, *Phys. Rev. B* **51**, 11501 (1995).

<sup>29</sup>E.g., V. G. Bhide, D. S. Rajoria, G. R. Rao, and C. N. R. Rao, *Phys. Rev. B* **6**, 1021 (1972).

<sup>30</sup>E.g., K. Asai, P. Gehring, H. Chou, and G. Shirane, *Phys. Rev. B* **40**, 10982 (1989).